

Geophysical model of geological discontinuities in a granitic aquifer: Analyzing small scale variability of electrical resistivity for groundwater occurrences

Subash Chandra^{a,*}, Benoit Dewandel^b, Sushobhan Dutta^{a,c}, Shakeel Ahmed^a

^a IFCGR National Geophysical Research Institute, Council of Scientific and Industrial Research, Hyderabad-500606, India

^b BRGM, Water Division, Hard Rock Aquifers Unit, 1039, Rue Pinville 34000 Montpellier, France

^c FUGRO, Mumbai, India

ARTICLE INFO

Article history:

Received 17 April 2009

Accepted 8 June 2010

Keywords:

Electrical resistivity tomography

Quartz reef

Intrusions

Lineament

Granite aquifer

Groundwater

ABSTRACT

Geological discontinuities such as quartz reef, a common geological feature in hard rock terrain occurring as an intrusive body, has been investigated using geophysical methods in order to explore and map the potential aquifer. Electrical resistivity response of quartz reef intrusive in granite host rock has been studied using synthetic simulation for different physical conditions such as: (1) fresh intrusive body with no alteration at contacts, (2) fresh intrusive body with weathered-fissured contacts, and (3) also fissured intrusive body with weathered-fissured contacts. Electrical Resistivity Tomography (ERT) was carried out traversing across and along the quartz reef at Kothur village, Hyderabad, India. Based on the ERT results 11 bore wells have been drilled followed by yield measurement, litholog collection, and electrical resistivity logging. Geomorphology, ERT images, lithologs, resistivity logs and yield of the wells are found corroborating with each other. Deepening of the weathering fronts are confirmed along the contacts of the quartz reef and granite, which may qualify suitable sites for groundwater occurrence. This has been finally validated from the drilling results, where high yielding (18 m³/h) bore well found at low resistive zones within the quartz reef. The study has helped in preparing a 2D section of the structural set up of the quartz reef in granite host medium and finally revealed that the quartz reefs may provide potential groundwater zone. The distribution of electrical resistivity of the geological discontinuity is useful providing promising input to the groundwater flow model particularly in three dimensional.

© 2010 Elsevier B.V. All rights reserved.

1. Introduction

Groundwater is the major source to supply the water needed for industrial, agricultural and domestic purposes and hence largely contribute to the economical development of such regions, especially for those exposed to arid and semi-arid climatic conditions, where the surface water resource is limited. The increasing stress on groundwater exploitation in such areas causes decline in its level consequently confining the flow to deeper weathered/fractured zones and thus making the situation alarming.

Aquifers in hard rock are complex in nature and are subjected to high variability of the hydrogeological parameters. Granitic terrains are normally traversed by lineaments such as quartz vein/reef, pegmatite veins, dolerite dykes, etc. that makes the groundwater dynamics more complex and hence, their characteristics become more important to understand the hard rock aquifer set up.

The lineaments play an important role in the groundwater dynamics and it act as indicator to locate the groundwater resources. Various

attempts have been made by several researchers to characterize the lineaments for their groundwater potentiality. Lattman and Parizek (1964) mapped linear feature (fracture traces) on stereo pairs of aerial photographs in the Eastern United State and subsequently showed the correlation between well productivity and distance to the identified features. The relationship of groundwater with lineament and fractures was studied by Mabee et al. (1994); Kresic (1995); Sander et al. (1997); Magowe and Carr (1999); Krishnamurthy et al. (2000) and agreed that a high density of lineament is, in general, indication of presence of groundwater. Hung et al. (2004) suggest that the fractured rock could be analyzed by studying lineaments with lineament indices. Owen et al. (2003) has correlated the yield of the bore wells with the distance to any aeromagnetic lineament and found a negative exponential relationship between them. Thus, for past few decades lineament mapping with remote sensing data especially in areas with igneous and metamorphic rocks of poor primary porosity (commonly referred as hard rock terrain) have been focus measurement for targeting well sites despite with varying success rates. Chandra et al. (2006) studied lineament such as dolerite dyke and major fractures running along the river/stream course and showed that lineament need not to be always potential or non potential to the groundwater. They have demonstrated that the geophysical characterization helps in understanding about the

* Corresponding author.

E-mail addresses: schandra75@gmail.com, chandra_s75@ngri.res.in (S. Chandra).

potentiality. Sander (2007) expressed that in real world, the best site for potential well may be far away from the lineaments, or lineament should be avoided or there is really nothing linear available in area where it is needed. Hence there is need of detailed characterization of lineaments and its validation for the groundwater potentiality.

Numerous kinds of lineament are discussed in the literature such as geologic lineament, tectonic lineament, photo lineament, etc. Even geologic lineaments are also consists of various kinds of features such as fracture, buried channel, intrusive (i.e. pegmatite, quartz reef and dolerite dyke) etc. and hence their characteristics also vary. Specific studies are needed for detailed investigations in real life problem. Also these structures that play crucial role for aquifer system in hard rocks have mostly been dealt geologically, needed to be investigated for their geophysical behavior and a combined investigations provide useful result. A Quartz reef, 20–30 m thick lineament, traversing N–S direction in granitic terrain near Hyderabad in Andhra Pradesh (India), has been studied in this paper.

Geomorphological, geophysical and hydrogeological studies have been carried out at quartz reef sites at Kothur village (hereafter termed as Kothur quartz reef) near Hyderabad (India). To validate the above results another site has been studied at ~5 km north near Indo-French research Project bore well number 1: hereafter termed as IFP-1 quartz reef site. Fig. 1 represent location of experimental sites i.e. Kothur and IFP-1 quartz reefs.

It is assumed that the quartz reef and granite contact is weak zone due to presence of cracks/fractures developed while intrusion. Water infiltrates along this zone and facilitate the weathering. Therefore, the contact can be a groundwater potential zone. The weathering and fissuring of the granite at contact zone causes swelling and hence consequently fissuring get developed in the surroundings. Thus main quartz reef body could also be fissured/fractured provided it is susceptible to fracturing. The quartz reef can also be groundwater potential provided it is well connected with the contact zone through open fracture network.

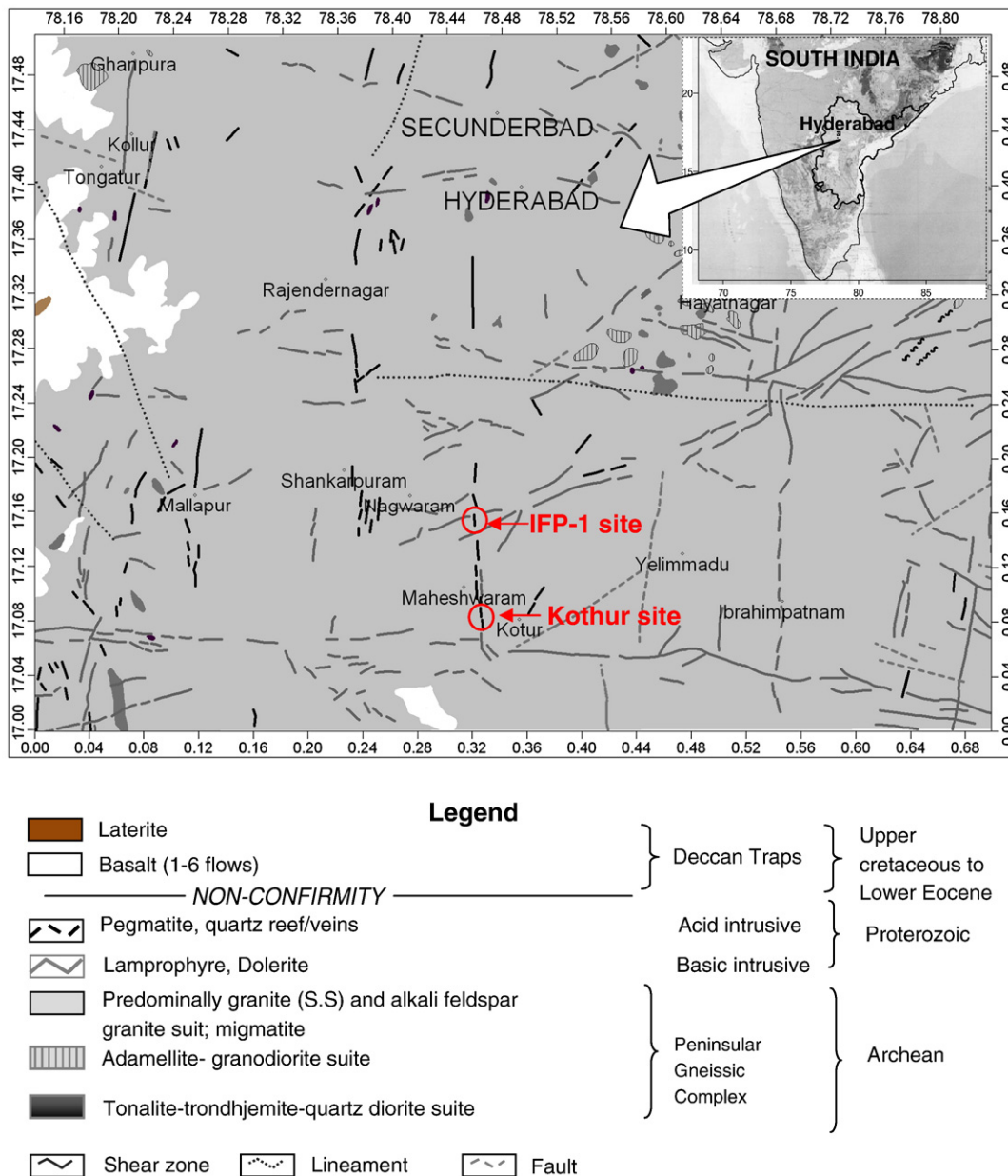


Fig. 1. Location map of study area: Kothur and IFP-1 quartz reef sites.

2. Granitic hard rock aquifer

The hydrogeological set up in the crystalline hard rock and its characteristics have been described by various researchers such as Davis and Turk, 1964; Tardy, 1971; Eswaran and Bin, 1978; Ledger and Rowe, 1980; Chilton and Smith-Carington, 1984; Acworth, 1987; Pickens et al., 1987; Nahon, 1991; Wright, 1992; Chilton and Foster, 1995; Sharma and Rajamani, 2000; Chigira, 2001; Begonha and Braga, 2002; Kuusela-Lahtinen et al., 2003; Dewandel et al., 2006. However, as this paper deals with the geological discontinuity of hard rock aquifer, a brief description about the essential and relevant features of hard rock system are described here.

In general, the hard rock aquifers, developed due to weathering and fracturing of basement rock, occupy the few tens of metres below ground surface. The hydrogeological characteristics (e.g., hydraulic conductivity and storage) of the covering weathered mantle (saprolite or alterite) and the underlying bedrock are derived primarily from the geomorphic deep weathering processes (Wyns et al., 1999; Taylor and Howard, 2000). Recent research on hard rock lithological setup (Wyns et al., 1999, 2004) depict a typical weathering profile (Fig. 2) comprised of multilayers (i.e. sandy regolith, laminated, fissured and fresh granite layers) having specific hydrodynamic properties individually. The multilayers all together (where and when saturated with groundwater) constitute a composite aquifer. The weathering of the mother rock results in the formation of fissured layer, generally characterized by 2 sets of sub-horizontal and sub-vertical fissures, where density decreases with depth (Houston and Lewis, 1988; Howard et al., 1992; Dewandel et al., 2006) and assume the Transmissivity function of the composite aquifer (Chandra et al., 2008). Variation in the thickness of these layers results in compartmentalizations of the granitic aquifer, even within a watershed (Ahmed et al., 1995).

The fresh basement, an impermeable layer, is permeable only locally, where tectonic fractures are present. The density of tectonic fractures is much lower than the within the fissured layer and hence basement as impermeable and of very low storativity (Maréchal et al., 2004). In addition to this the presence of lineaments such as rivers streams, buried channels, quartz and pegmatite veins/reefs, dolerite dykes, etc., makes further complex the groundwater dynamics.

3. Studies carried out

An integrated study consists of topographical mapping using Differential Global Positioning System (DGPS) of quartz reef site, forward 2D resistivity modeling from synthetic data, ERT survey,

drilling of experimental bore wells, litholog collection, yield measurements, and electrical resistivity logging have been carried out.

3.1. DGPS surveys

Differential Global Positioning Systems (DGPS) gives differentially corrected x, y and z coordinates with reference to the known bench mark and hence enables to bring all the observation points to a common reference level viz. mean sea level (in the present case). Real time kinematics survey was carried out using DGPS (Trimble R7) at Kothur and IFP-1 quartz reef sites covering $\sim 500 \times 500 \text{ m}^2$ area to represent topographic elevation (Fig. 3). The vertical resolution of the data obtained from this system is within sub cm (say $\pm 5 \text{ mm}$) accuracy. Data points were selected based on the topographic gradient for example dense data were taken over the quartz reef and its vicinity, and scattered data away from the quartz reef. The topography away from the quartz reef is more or less flat. In addition to this some of the ERT profiles each with 48 points, bore wells were also covered. Total 347 and 125 DGPS points were collected at Kothur and IFP-1 sites respectively. Data was used to prepare the topographic contour maps, which are found varying from 616 m to 631 m amsl, and 593 m to 609 m amsl at Kothur and IFP-1 quartz reef sites respectively.

3.2. Synthetic 2D resistivity modeling

Normally electrical profiling survey is preferred for characterizing a linear feature, where large number of measurements use to take with different electrode spacing manually and thus require huge amount of work as well as become time consuming task. The development in the resistivity technique as electrical resistivity tomography (ERT) facilitate to map 2D and 3D resistivity distributions of subsurface bodies reliably and require less time (Barker, 1978; Griffiths et al., 1990; Loke and Barker, 1996; Barker et al., 2001). Forward modeling have been attempted here to see the geoelectrical response of the quartz reef intrusive in the granitic host medium and design the experiment particularly electrode configuration, spacing and depth of investigations. A 470 m long and 130 m deep 2D physical model was prepared representing the actual field conditions. Wenner–Schlumberger configuration with 5 m and 10 m electrode spacing were used to generate apparent resistivity data using RES2DMOD. Fresh as well as fissured quartz reef intruded in the granite host medium with fresh as well as weathered-fissured contacts have been simulated.

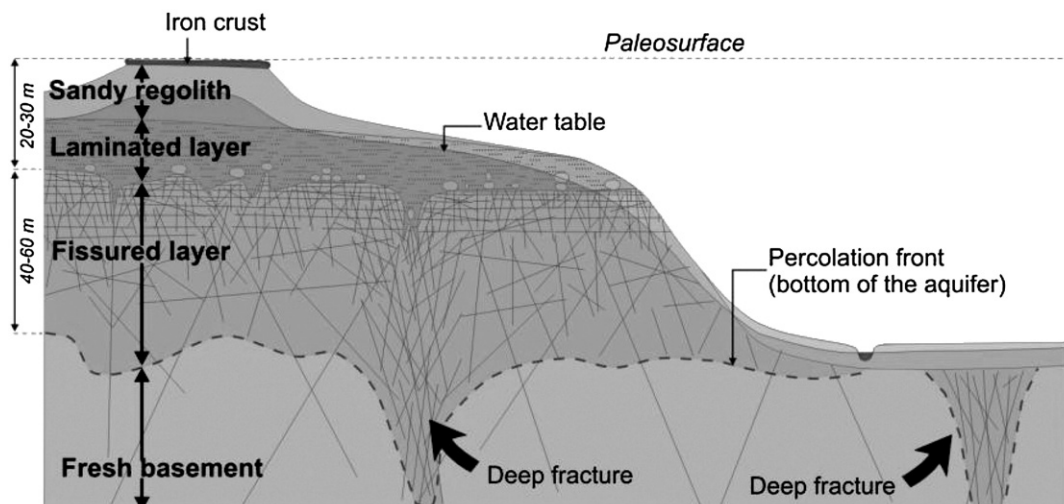


Fig. 2. Idealized single phase weathering paleoprofile in a hard-rock, crosscut by the current topography (Wyns et al., 1999, 2004).

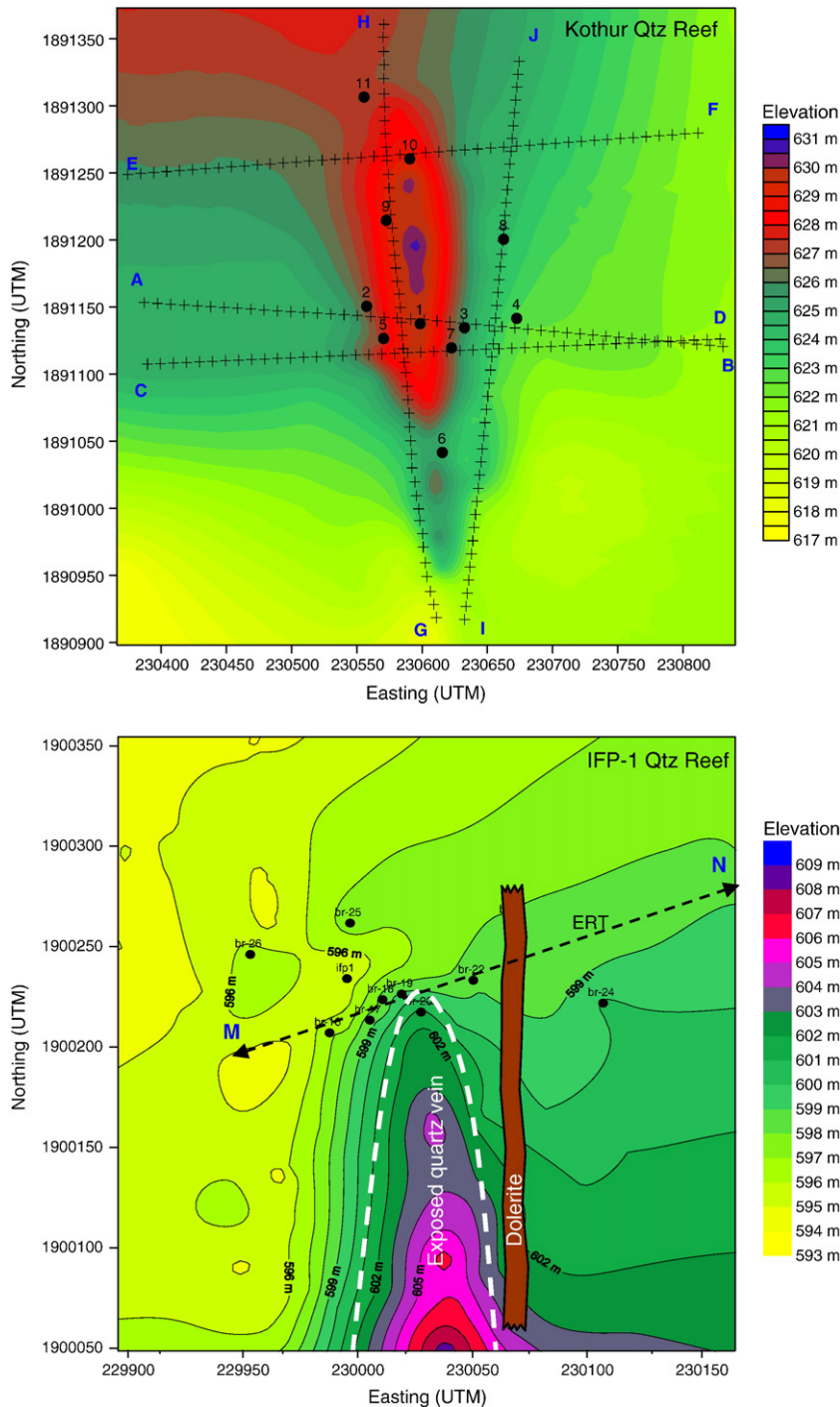


Fig. 3. Location map of quartz reef sites along with ERT profiles and bore wells.

Although, it's not possible to get horizontal stratified layers in granite, but here various geoelectrical layers are considered with the logic that the degree of alteration in the granite reduces with depth resulting in reduction of the volumetric percentage of water with depth that causes rise in resistivity. Or in other words resistivity of these layers successively increases for soil, laminated, weathered-fissured, fissured layers and fresh granite basement. Thus a layered succession for electrical resistivity can be considered even in the granitic medium too. The blocks lying in the 30 m thick band vertically sitting at centre to represent quartz reef has been assigned 1280 Ω m resistivity. Resistivity assigned to soil, laminated, weathered-fissured, and fissured granite are respectively 40, 160, 320 and 640 Ω m (Fig. 4a).

However, resistivity assigned to blocks in the bottom row for the granite basement is similar to the quartz reef. Since the granite is fresh and compact at deeper level, it will behave electrically same as quartz reef. In contrary to this soil resistivity could be comparatively higher than the weathered zone during the dry climatic season as soil water gets evaporated. Assuming the wet soil condition a vertical fresh quartz reef intruded in granite is taken and synthetic 2D apparent resistivity data is generated using RES2DMOD (Loke, 2001). Exercise has also been done of adding random errors varying from 2–20% to the generated synthetic data. The resultant data were inverted using RES2DINV for getting true resistivity. Five typical models to show the electrical response of quartz reef intrusive in granite are shown in Fig. 4.

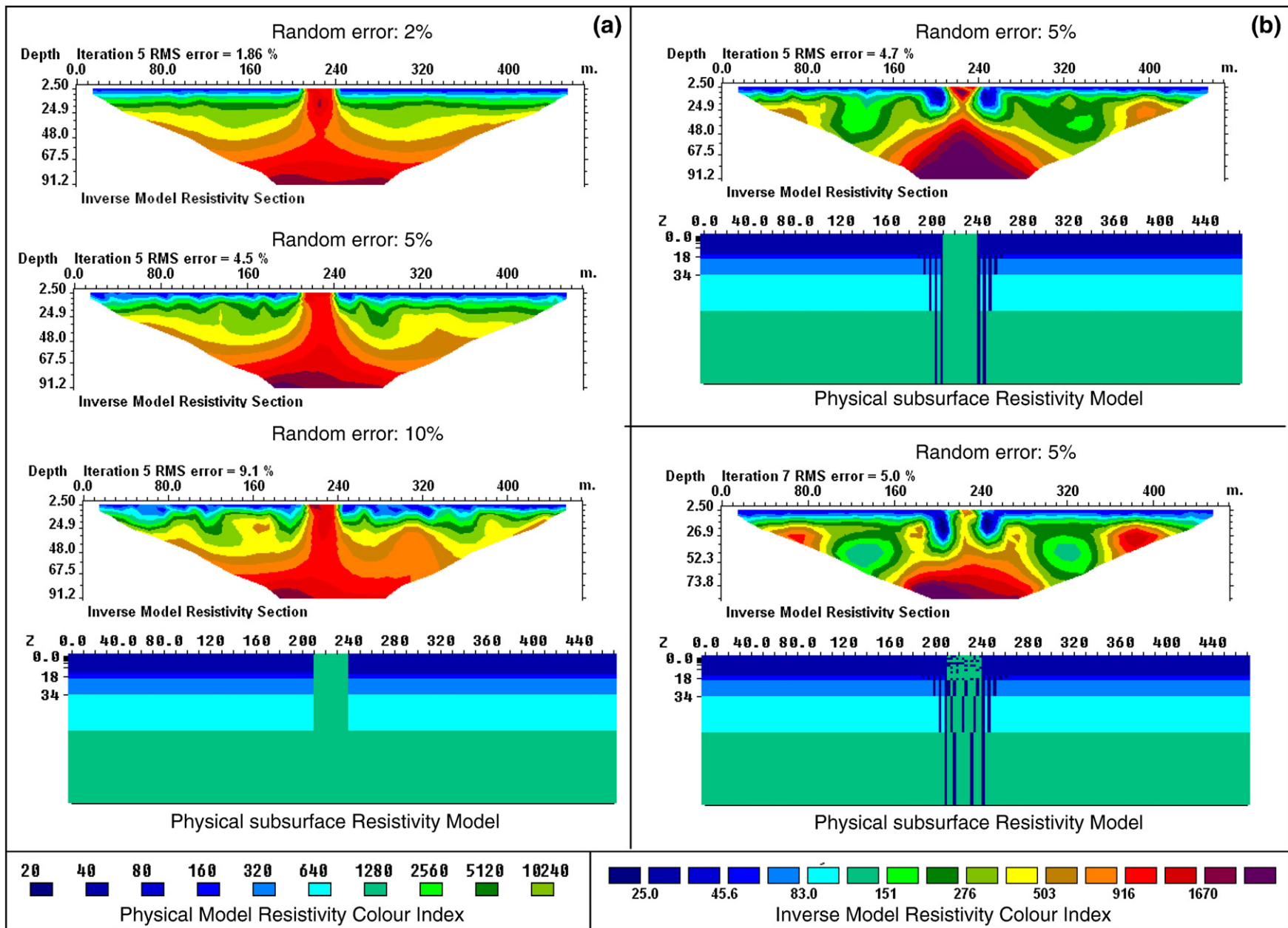


Fig. 4. Synthetic ERT model over (a) fresh quartz vein, (b) fresh quartz vein with weathered-fissured granite contacts and (c) fissured quartz reef with weathered-fissured granite contact.

It is quite obvious that lesser the random noise, closer the inverted resistivity section to the physical model which was achieved here. The inverted images in Fig. 4a present the electrical response of fresh quartz reef intrusive in granite host medium composed of homogeneous stratified geoelectrical layers. For 2% random error added in synthetic data, the inverted image revealed more or less stratified geoelectrical layers. The 1280 Ωm resistive and 30 m (210–240 m on lateral scale) thick quartz reef appeared with high vertical resistivity anomaly ranging from 503 to 1237 Ωm . Similar to the homogeneous stratified geoelectrical layers of granite in physical model, inverted image also has reproduce similar electrical resistivity response except than over the quartz reef and just its vicinity (i.e. within 10 m).

The geoelectrical layers appeared with ripples when random error was increased to 5% or more. With 5% random error ripples are seen roughly up to 20 m depth (Fig. 4a). Whereas 10% and 20% random error affected geoelectrical layers with rippling greater depth (i.e. >20 m). Our zone of interest is 20–70 m, as aquifer lies in this horizon in the study area. Therefore 5% random error is acceptable. In Fig. 4a typical images are shown with random error of 2, 5 and 10%.

The Fig. 4b represents the synthetic simulation with 5% random error over quartz reef intrusion with weathered-fissured contacts. The blocks along the contacts were assigned 20 Ωm resistivity to represent the weathering-fracturing filled with water. Lowering of two lobes of $\sim 25 \Omega\text{m}$ along the contacts was seen, which is nothing but the response of weathering-fracturing along the contacts.

Considering that the weathering along the contact zones causes swelling that produces tensile forces acting on the surroundings and developing fissures/cracks, some blocks within the quartz reef were assigned 20 Ωm resistivity. Significant resistivity response (i.e. lowering of resistivity at the contact) can be seen of fissured quartz reef with weathered-fissured granite contact in Fig. 4c. Resistivity of quartz reef in the inverted image has further reduced falling in the range of 50–679 Ωm . Although, there should be some dry fractures (that increases the resistivity) also because of non-interconnection, but the synthetic simulation has been carried out assuming that most of the fractures are saturated with water. Of course, the fractures could be considered saturated with water during rainy season or during post monsoon period and getting dry (at shallow level) during summer and hence rise in the bulk resistivity.

The synthetic simulation has finally helped in understanding the electrical signature of the quartz reef intrusive in granite with varied hydrogeological conditions. It was decided to carry out ERT with Wenner–Schlumberger array keeping 10 m electrode spacing.

3.3. Field ERT and resistivity logging

Depending on the accessibility of the area, three ERT profiles (Wenner–Schlumberger configuration with 10 m electrode spacing by Syscal Jr Switch 48 system) running across and two profiles at contacts running parallel to the Kothur quartz reef were carried out (Fig. 3). Clay mixed with salt water were kept over the exposures to plant the electrodes as well as to reduce the contact resistance. However, the contact resistance still carries some effect that probably has amplified the resistivity and also the RMS error while inversion. The effect of the resistance of the contact material used will, in any case, be negligible due to large electrode spacing. Some data points having anomalous standard deviation (i.e. $>>5$), were removed as bad data quality. Profile topography has been included in the measured apparent resistivity data for elevation correction before inversion.

The inverted image of the field data were studied and 11 bore wells viz., IFP30/1 to IFP30/11 were drilled with depth varying from 48–84 m where the deepest well is drilled on the quartz reef to validate the ERT results. The spatial distribution of bore well is given in Fig. 3.

To obtain the resistivity of the various formations, some of these bore wells were logged in the water saturated portion (i.e. between

water table and bottom of the well) with the help of special logging tool (sonde) fabricated at Indo-French Centre for Groundwater Research, NGRI, Hyderabad (India). It works on the two-electrode configuration method, where one each current and potential electrodes were kept comparatively at infinite distance on the ground. However, another set of one each current and potential electrodes was fixed on the sonde with one meter electrode separation. Log measurement was taken at every 0.5 m interval below the casing in zone of saturation and calculated apparent resistivity (ρ_a) by using Eq. (1) (Keller and Frischknecht, 1966):

$$\rho_a = 4\pi r \frac{\Delta V}{I} \quad (1)$$

where r , ΔV and I are respectively electrode spacing (m), measured potential difference (mV) and injected current (mA). Using Schlumberger's (1955) resistivity departure curve, formation resistivity was calculated for each well. Topography elevation of observation points has been incorporated to bring the images with reference to the mean sea level.

4. Results and discussions

Quartz reef is well exposed i.e. $\sim 2\text{--}7$ m elevated from the surrounding. Both the locations i.e. Kothur and IFP-1 fall on the major quartz reef traversing in N–S direction. In general, topography is sloping towards east. Although number of synthetic ERT simulations were attempted with 5 m and 10 m electrode spacing, but ERT with 10 m spacing was found suitable to the present problem and carried out ERT surveys with 10 m spacing. Since the topography is elevated over the quartz reef, electrode elevation data above the mean sea level were introduced to the measured apparent resistivity data for applying the elevation correction.

The field ERT profiles running across the Kothur quartz reef have shown almost the expected response similar to the synthetic model. The observed cumulative resistivity of exposed quartz reef in the perpendicular ERT profiles AB, CD and EF found in the range of 1000 to 30,000 Ωm . Although, this is abnormally high compared to surrounding top layer that are found in the range of 10–100 Ωm over the granite (Fig. 5), but is much low compared to fresh quartz crystal resistivity i.e. 10^{12} to $3 \times 10^{14} \Omega\text{m}$. Weathering/fracturing of quartz reef and mixing of other materials such as clay, water, etc might be responsible for this reduction.

Even though the quartz reef exposure shows same width on the surface, but the resistivity obtained over this is not exactly same for all the profiles. These variations are probably indication of the spatial change in the degree of weathering/fracturing in the quartz reef body. Resistivity of the weathered and fissured quartz reef ranges from 200 to 400 Ωm . Resistivity anomaly ranging from 30–300 Ωm could also be seen over the contacts (i.e. on either side of quartz reef at 200–220 m and 250–270 m on ERT profile). This is low compared to the neighboring blocks. Comparing the images to the synthetic resistivity model, the relatively conductive anomaly over the contacts could be inferred as deepening of weathering/fracturing front.

The ERT section CD has shown abnormally high resistive (i.e. 9000 to 28625 Ωm) vertical anomaly continuing to bottom indicating the compact quartz reef, but the discontinuity were observed in the sections AB and EF at mid level. Such discontinuity could be inferred as occurrence of weathering and fissuring in the quartz reef body itself as it is found similar to the synthetic model with weathered-fissured contact and quartz reef body.

Resistivity of granite basement is found in general $\geq 3000 \Omega\text{m}$ in this area (Chandra, 2006). With the above consideration on average basement is found at ~ 610 m, 600 and 590 m in the ERT images AB, CD and EF respectively. These basement depths were

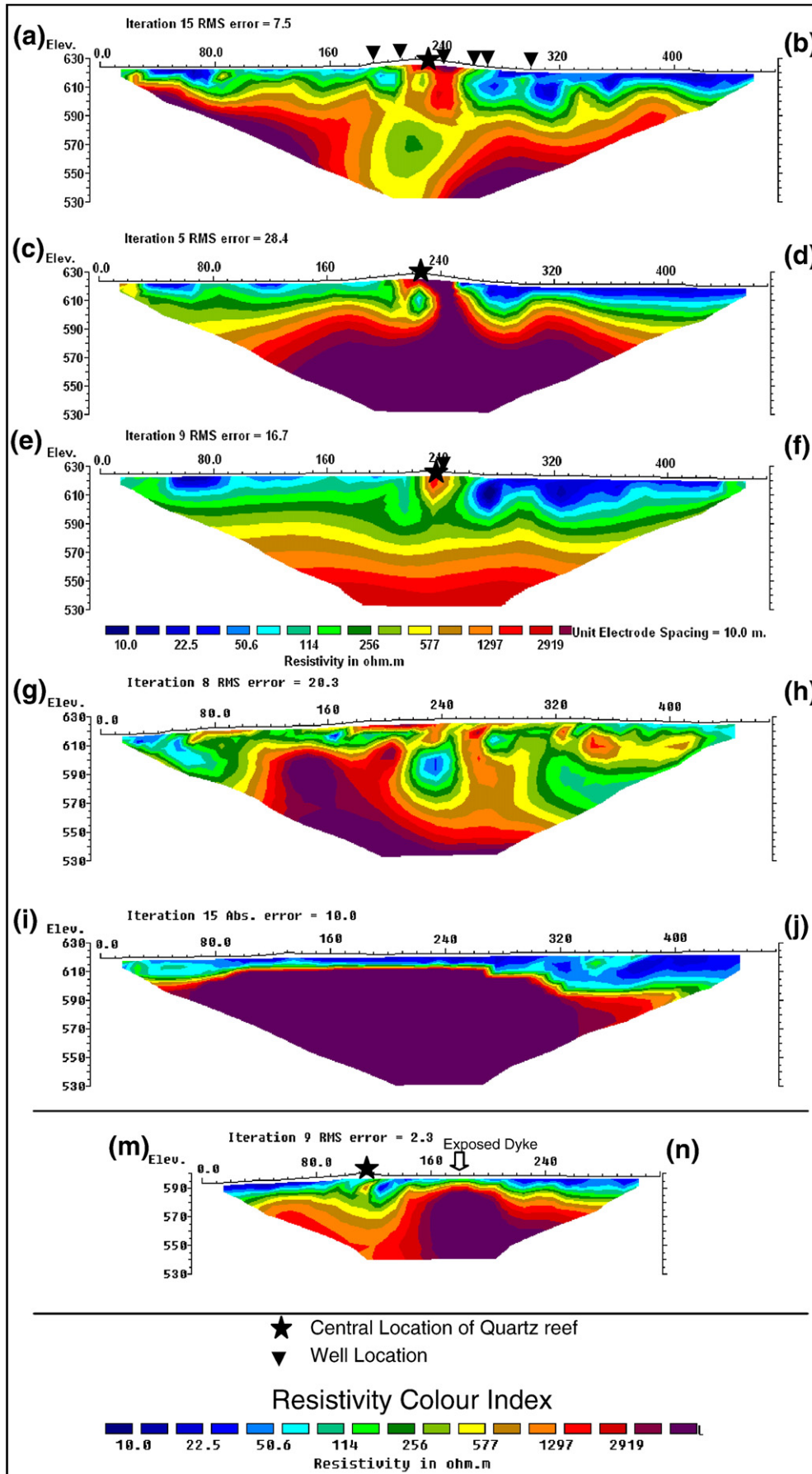


Fig. 5. Field ERT images ab, cd and ef across and gh and ij along the Kothur quartz reef and mn across profile over IFP1 quartz reef.

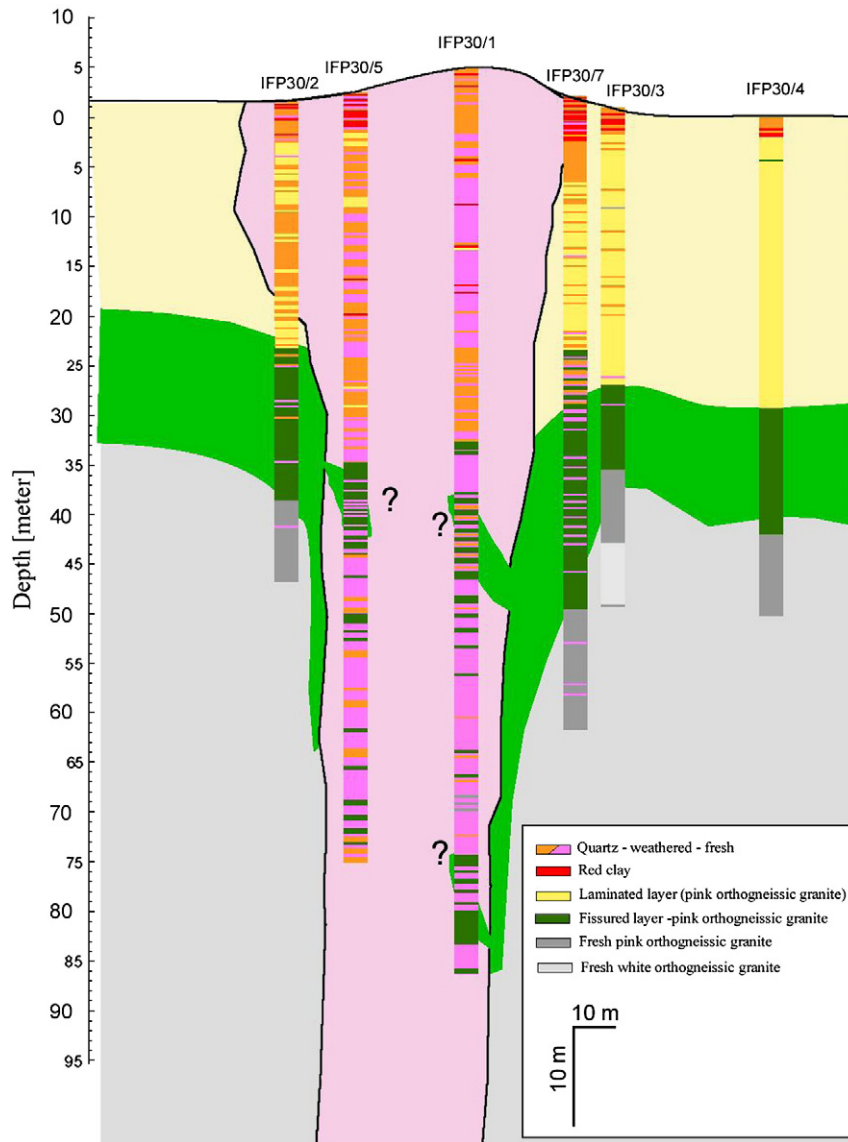


Fig. 6. Litholog of IFP 30/1-30/5 and 30/7 bore holes.

further confirmed by the GH and IJ roughly parallel ERT profiles to the reef by revealing a regional lowering of basement towards north.

To have an idea of lithological characteristics at X–Y plane, resistivity at 610 m amsl from all ERT profiles were taken and prepared resistivity contour map. The equi-resistive lines are elongated in N–S direction

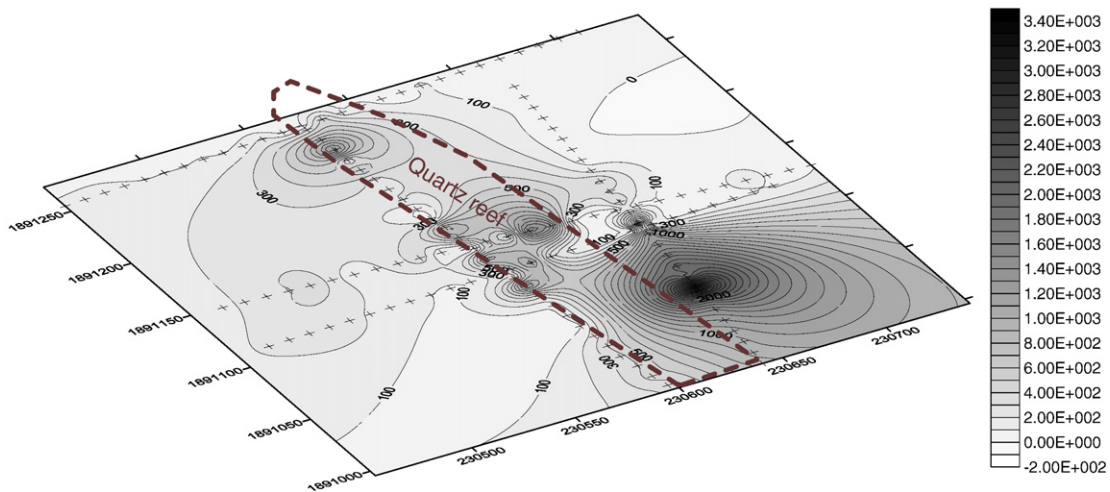


Fig. 7. Horizontal 2D resistivity distribution at 610 m amsl of Kothur site.

indicates major fracture alignment running parallel to quartz reef (Fig. 6). Probably the dense weathering-fissuring at the contact has resulted equi-resistive elongation in N–S direction over it. Thus, in other words, groundwater will dominantly flow towards north.

Geophysical results were confirmed with the lithologs of the drilled wells falling in a N–S line i.e. IFP-30/1, 30/2, 30/3, 30/4, 30/5 and 30/7 corresponding to ERT section AB (Fig. 7). The quartz reef has shown weathering and fissuring effects in the rock cutting and thus satisfies the hypothesis of generation of tensile fracture due to swelling along the contacts. The deepest (i.e. 84 m) well 'IFP 30/1' lying in the centre of the quartz reef has shown weathering fracturing effects in the rock cuttings till bottom. Based on the lithologs, a conceptual hydrogeological set up across the quartz reef has been prepared that indicates laminated layer (pink orthogneissic granite), fissured layer (pink orthogneissic granite), fresh pink orthogneissic granite, fresh white orthogneissic granite and quartz-weathered/fresh (Fig. 7). Another four drilled bore wells correspond to the other ERT profiles.

Resistivity log plot of the bore wells i.e. IFP 30/1, 30/2, ..., 30/5 falling in a line traversing in N–S direction across the quartz reef, are given in Fig. 8a. In general, the starting resistivity at ~610 m amsl found in the range of 10–100 Ω m and maintains more or less same resistivity further ~20 m downward. However, it starts suddenly rising and reaches to 3000 Ω m or even more. The gradient of rise after 3000 Ω m either stops (eg. IFP 30/3) or slow down (e.g. IFP 30/4 and 30/5) indicating the logger reached to the fresh granite basement zone. To have better understanding these log results were utilized to prepare 2D resistivity distribution map. The granite basement level were found, from west, in the wells IFP-30/2 and 30/5 at 588.36 and 587.96 m respectively and in the wells IFP-30/4 and 30/3 (from east) respectively at 590.80 m and 591.64 m amsl. However log resistivity in the central well (IFP 30/1) lying within the quartz reef body does not attain 3000 Ω m. Mostly resistivity is found around 300 Ω m till bottom indicating deep weathering/fracturing (Fig. 8).

The map shows electrically conductive zone at the contacts of quartz reef and granite as well as over the quartz reef, or in other words, deepening of the basement towards the contact (Fig. 8). In addition to this the basement on the western contact of the quartz reef is deeper (i.e. at ~588 m amsl) than the eastern contact (i.e. at ~590 m amsl). As per the topography the western contact lies in the upstream part, which usually has longer residence period leading deeper weathering-fissuring than the downstream contact.

The contact plane between quartz crystals may be acting as conduits to facilitate the water percolation even quite deeper compared to the contact zones and hence reduction the electrical resistivity (refer resistivity log of IFP 30/1 in Fig. 8) has been achieved. The quartz reef also can be inferred as is more susceptible for fracturing than the granite because of its crystallography. Yield of the bore wells were found well corroborating with the above results, however, yield was found more towards north as aquifer thickness is comparatively higher as well as resistivity is low that is the indication of high degree of weathering and fissuring (see profiles GH & IJ in Fig. 5).

The bore wells IFP 30/4, 30/5 and 30/11 falling around the contact zone have shown yield 7.5, 8, and 10.85 m³/h respectively, which is quite logical. In general, basement is dipping towards north; hence water accumulation will be more in north. Since aquifer thickness is increasing towards north and resistivity is comparatively decreasing (i.e. increase in degree of weathering and fissuring), yield of the bore well is expected to be more that has been observed here. This was confirmed by the bore well IFP-30/10 lying in quartz reef with highest yield (i.e. 18 m³/h) among all.

Thus all the results from topography, synthetic simulation, field ERT, litholog, logging results and yield of bore wells found well corroborating with each other and supporting the assumption/hypothesis of deepening of weathering/fracturing fronts over the contacts as well as generation of fractures inside the intrusive body, which turn into groundwater potential zones.

The second quartz reef site at IFP-1 has shown almost similar response. In fact this site is a bit more complex because of nearby parallel

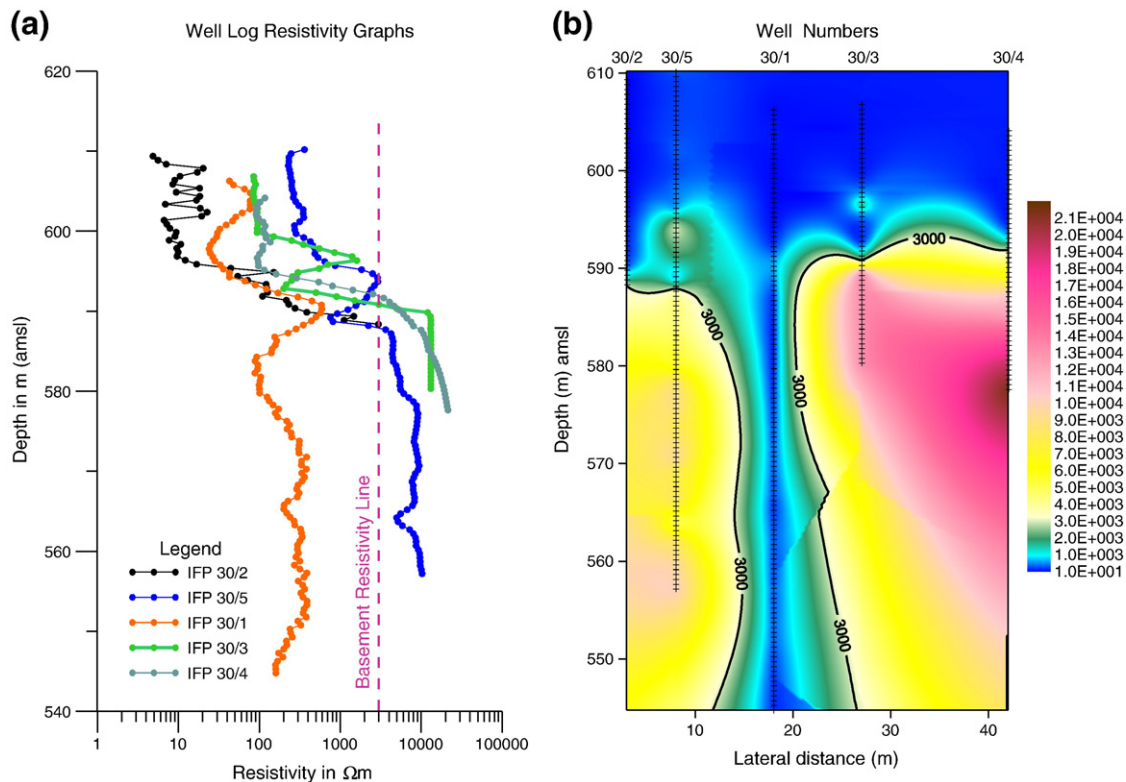


Fig. 8. (a) Electrical resistivity log curves and (b) resistivity map obtained from the wells: IFP 30/2, 30/5, 30/1, 30/3 and 30/4 running across the quartz reef at Kothur, Hyderabad.

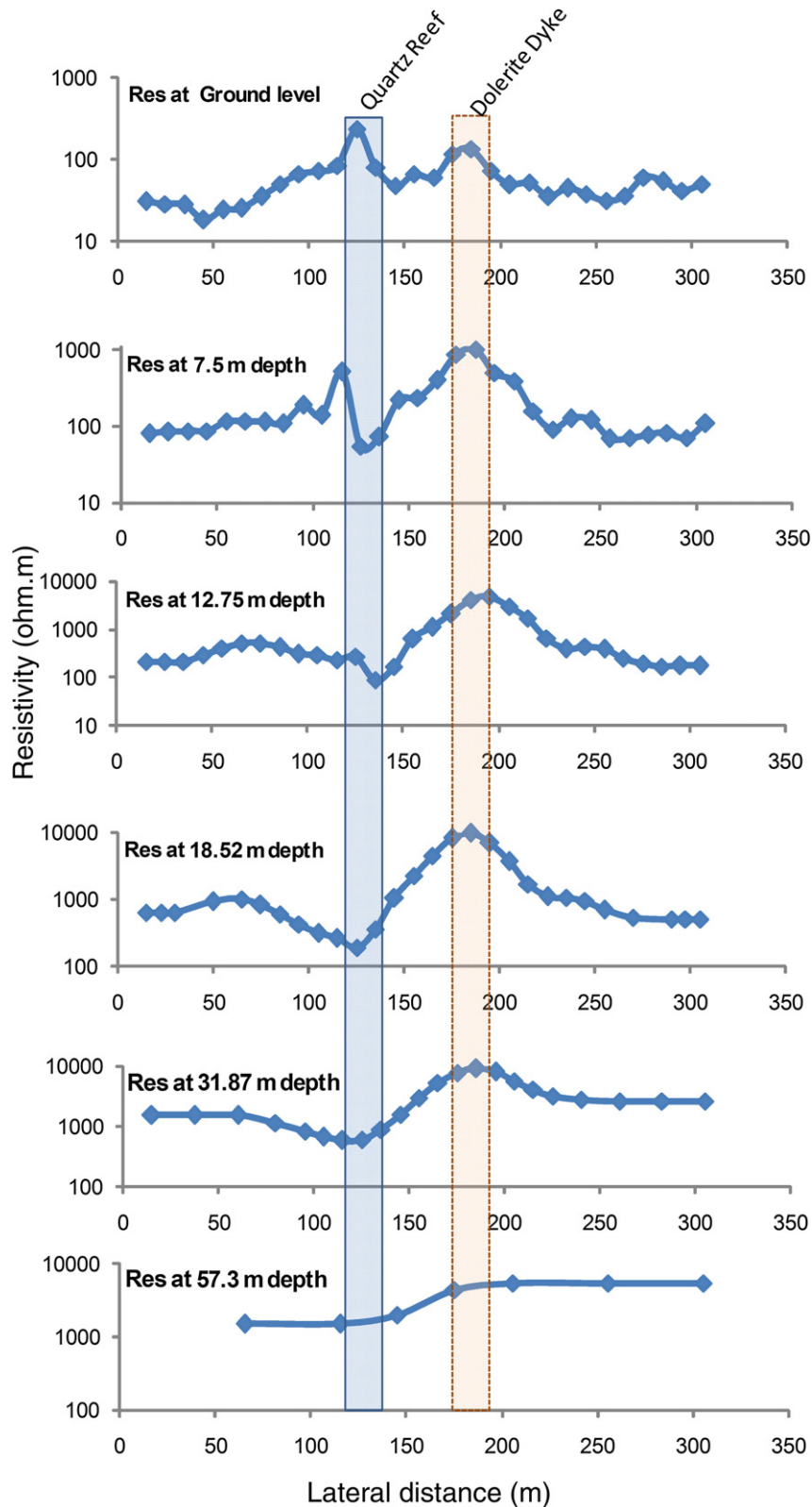


Fig. 9. Lateral resistivity distribution at IFP-1 site.

traverses of dolerite dyke (Fig. 3). The ERT profile MN crosses at the tapering portion of quartz reef. However, quartz reef impression can be seen in the form of relatively high resistivity ranging from ~500 to 600 Ωm at 120 m of MN profile at shallow level surrounded by low resistivity (i.e. 100–200 Ωm) blocks (Fig. 5). An anomalous zone can be seen between 165 and 190 m on lateral scale. This zone offered

resistivity in the range of 50 to 500 Ωm up to top 10 m whereas further down the range shifts to 500–5000 Ωm . This is the impression of dolerite dyke with weathering at the top.

Though the quartz reef and dolerite dyke both are intrusive, but have contrast characteristics as revealed by Fig. 9 consists of lateral resistivity distribution profiles at different depth levels prepared from

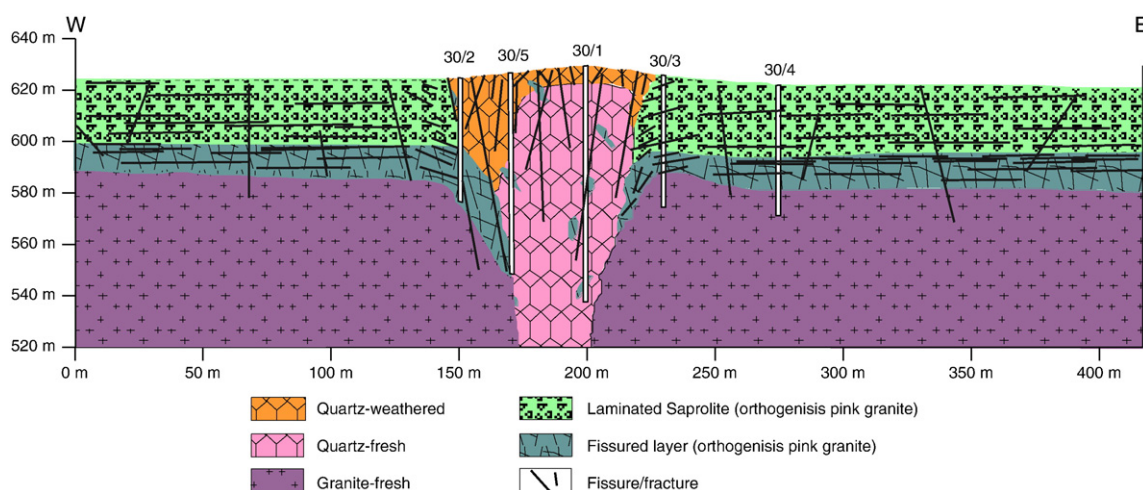


Fig. 10. Lithological set up of quartz reef in granite at Kothur, Hyderabad.

ERT data at IFP-1 quartz reef site. Resistivity distribution over exposed quartz reef at ground level are found higher (i.e. 234 Ωm) than resistivity of dolerite dyke (i.e. 136 Ωm) at 185 m. However, further going downward at depth level 12.75 m, resistivity of quartz reef at 115 m distance on profile has increased to 516 Ωm simultaneously, the resistivity of the dolerite dyke has also increased to 1022 Ωm . Such contrast variation in resistivity over these two intrusives are indication of contrast characteristics of weathering and fissuring as well as its variation in mineralogical composition that is responsible for electronic current conduction. Quartz reef is more susceptible for fissuring, whereas spheroidal weathering is common feature over dolerite. The earlier work of Chandra et al. (2006) on ERT response over dolerite dyke intruded in granite indicates that the upper portion of such intrusives are weathered at shallow level (up to 8 m) reflected as low resistivity and further downward it is compact and shown as high resistivity.

Since ERT profile passes at pinch out portion of quartz reef, it can't be expected at further deeper level, but still its impression can be observed in the form of lowering of resistivity at 115 m lateral distance downward up to 57.3 m (Fig. 9). As quartz reef is intrusive, number of cracks are expected to be developed, which facilitate to percolate surface water and further leads to weathering.

Integrating the results of ERT, resistivity log, litholog, etc, a 2D geological set up of quartz reef in granite host medium has been prepared (Fig. 10). This model is quite similar to hydrogeological model given by Wyns et al. (1999) with additional intrusive of quartz reef. The model shows weathered quartz at top and the deepening of weathering-fissuring over the contacts. However, more refined model can be prepared including some more studies with dense sampling.

There have been many studies investigating the aquifer parameters from geophysical method in order to support essential input to groundwater flow model (Kelley, 1977; Mazac et al., 1985; Huntley, 1986; Frohlich et al., 1996; Singhal et al. 1998; Niwas and de Lima, 2003; Chand et al., 2004; Singh, 2005; Chandra, 2006 and Chandra et al., 2008). Thus the 2D/3D resistivity distribution of the geological discontinuities is useful parameter to characterizes the hydrodynamic properties of the hard rock system.

5. Conclusion

The present studies conclude that the surface geophysical method particularly ERT is an efficient tool to provide detailed distribution of electrical resistivity to characterize the lineament such as quartz reef in granite host rock. A thorough mapping along and across the quartz reef by electrical resistivity method has provided the small scale parameter variation correlating with the degree of weathering/

fissuring at various depths. The quartz reef intrusive in granite rock can be very useful for locating a potential aquifer. The contact zones of quartz reef may provide potential groundwater zone as deepening of the weathering front is established with reasonable accuracy. Although the intrusive always create a shear zones usually favourable for groundwater occurrence and flow but the present investigations have provided a detailed subsurface scenario quantifying the variability even at small scale. The groundwater flow from upstream side to downstream get accumulated in the zone and make favourable location for siting a high yielding well. The well IFP-30/10 drilled at the centre of the reef has proved as one of the highest yielding well at Kothur quartz reef site. Thus quartz reef can also be potential groundwater zone provided it is well connected with the contact zone through open fractures.

Study also concludes that ERT measurements at the contact running parallel to the reef must be carried out before the drilling because the degree of weathering/fracturing as well as basement depths varies. The deeper basement zone with high degree of weathering/fracturing qualifies potential aquifer site. Geological set up of Kothur quartz reef has been prepared based on the overall results.

Although quartz reef and dolerite dyke both are intrusive in granite host rock, but have contrast characteristics in weathering and fracturing leading to a different role for groundwater dynamics. The weathering/fracturing were limited to ~8 m in the granite, whereas it is found up to 85 m depth in quartz reef.

The investigation has added extremely useful information at a detailed scale that usually not practiced during geological investigations. For examples siting the most yielding bore well at the centre of the quartz reef was not possible by simple observations or only geological investigation alone. Degree and depth of weathering of such younger formations and preparing its subsurface model are unique findings through geophysical method.

Acknowledgement

This study has been carried out at the Indo-French Centre for Groundwater Research (IFCGR), a joint centre of NGRI, India and BRGM, France. The authors wish to thank the Ministry of External Affairs of both the countries for their kind support and cooperation. We are thankful to Director, NGRI, Hyderabad for his support, encouragement and according permission to publish this paper. The help extended by Dr. Dewashish Kumar during the field work is sincerely acknowledged. Special thanks to Md Ahmeduddin for his help in preparing the manuscript. Thanks to anonymous reviewer for their critical review that improved the paper quality.

References

- Acworth, R.I., 1987. The development of crystalline basement aquifer in a tropical environment. *Q. J. Eng. Geol.* 20, 265–272.
- Ahmed, S., Sankaran, S., Gupta, C.P., 1995. Variographic analysis of some hydrogeological parameters: use of geological soft data. *J. Environ. hydrool.* 3 (2), 28–35.
- Barker, R.D., 1978. The offset system of electrical resistivity sounding and its use with a multi-core cable. *Geophys. Prospect.* 29, 128–143.
- Barker, R., Rao, T.V., Thangarajan, M., 2001. Delineation of contaminant zone through electrical imaging technique. *Curr. Sci.* 81 (3), 277–283.
- Begonha, A., Braga, M.A.S., 2002. Weathering of the Oporto granite: geotechnical and physical properties. *Catena* 49, 57–76.
- Chand, R., Chandra, S., Rao, V.A., Singh, V.S., Jain, S.C., 2004. Estimation of natural recharge and its dependency on subsurface geoelectric parameters. *J. Hydrol.* 299, 67–83.
- Chandra, S., 2006. Contribution of geophysical properties in estimating hydrogeological parameters of an aquifer. unpublished Ph.D thesis. BHU, Varanasi, pp. 176.
- Chandra, S., Ahmed, S., Ram, A., Dewandel, B., 2008. Estimation of hard rock aquifers hydraulic conductivity from geoelectrical measurements: a theoretical development with field application. *J. Hydrol.* 35, 218–227.
- Chandra, S., Rao, V.A., Krishnamurthy, N.S., Dutta, S., Ahmed, S., 2006. Integrated studies for characterization of lineaments to locate groundwater potential zones in hard rock region of Karnataka, India. *Hydrogeol. J.* 14 (5), 767–776.
- Chigira, M., 2001. Micro-sheeting of granite and its relationship with landsliding specially after the heavy rainstorm in June 1999, Hiroshima Prefecture, Japan. *Eng. Geol.* 59, 219–231.
- Chilton, P.J., Smith-Carington, A.K., 1984. Characteristics of the Weathered Basement Aquifer in Malawi in Relation to Rural Water Supplies. Challenges in African Hydrology and Water Resources, proc. Harare Symposium, July 1984, pp. 57–72.
- Chilton, P.J., Foster, S.S.D., 1995. Hydrogeological characterization and water-supply potential of basement aquifers in tropical Africa. *Hydrogeol. J.* 3 (1), 36–49.
- Davis, S.N., Turk, L.J., 1964. Optimum depth of well in crystalline rocks. *Ground Water* 2, 6–11.
- Dewandel, B., Lachassagne, P., Wyns, R., Maréchal, J.C., Krishnamurthy, N.S., 2006. A generalized 3-D geological and hydrogeological conceptual model of granite aquifers controlled by single or multiphase weathering. *J. Hydrol.* 330, 260–284.
- Eswaran, H., Bin, W.C., 1978. A study of deep weathering profile on granite in peninsular Malaysia: I. Physico-chemical and micromorphological properties. *J. Soil Sci. Soc. Am.* 42, 144–149.
- Frohlich, R.K., Fisher, J.J., Summerly, E., 1996. Electrical hydraulic conductivity correlation in fractured crystalline bedrock: Central Landfill, Rhode Island, USA. *J. Appl. Geophys.* 35, 249–259.
- Griffiths, D.H., Turnbull, J., Olayinka, A.I., 1990. Two-dimensional resistivity mapping with a computer-controlled array. *First Break* 8, 121–129.
- Houston, J.F.T., Lewis, R.T., 1988. Victoria province draught relief project, II. Borehole yield relationships. *Ground Water* 26, 418–426.
- Howard, K.W.F., Hughes, M., Charlesworth, D.L., Ngobi, G., 1992. Hydrogeological evaluation of fracture permeability in crystalline basement aquifers of Uganda. *Hydrogeol. J.* 1, 55–65.
- Hung, L.Q., Batelaan, O., San, D.N., Smedt, F.de, 2004. Lineament analysis for the groundwater in karst fractured rocks in the Suoimuoi karst catchment, Trans-KARST 2004. Proceedings of the International Transdisciplinary Conference on Development and Conservation of Karst Regions, Hanoi, Vietnam.
- Huntley, D., 1986. Relations between hydraulic conductivity and electrical resistivity in granular aquifers. *Ground Water* 24, 466–474.
- Keller, G.V., Frischknecht, F.C., 1966. Electrical methods in geophysical prospecting First Edition. Pregamon Press Inc.
- Kelley, W.E., 1977. Geoelectrical sounding for estimating hydraulic conductivity. *Ground Water* 15, 420–425.
- Kresic, N., 1995. Remote sensing of tectonic fabric controlling groundwater flow in dinaric karst. *Remote Sens. Environ.* 53, 85–90.
- Krishnamurthy, J., Mani, A., Jayaraman, V., Manivel, M., 2000. Groundwater resources development in hard rock terrain – an approach using remote sensing and GIS techniques. *Int. J. Appl. Earth Obs. Geoinf.* 2 (3/4), 204–215.
- Kuusela-Lahtinen, A., Niemi, A., Luukkainen, A., 2003. Flow dimension as an indicator of hydraulic behaviour in site characterization of fractured rock. *Ground Water* 41 (3), 33–341.
- Lattman, L.H., Parizek, R.R., 1964. Relationship between fracture traces and the occurrence of groundwater in carbonate rocks. *J. Hydrol.* 2, 73–91.
- Ledger, E.B., Rowe, M.W., 1980. Release of uranium from granitic rocks during in situ weathering and initial erosion (central Texas). *Chem. Geol.* 29, 227–248.
- Loke, M.H., 2001. Tutorial : 2-D and 3-D Electrical Imaging Surveys. , p. 118.
- Loke, M.H., Barker, R.D., 1996. Rapid least-squares inversion of apparent resistivity pseudosections using a quasi-Newton method. *Geophys. Prosp.* 44, 131–152.
- Mabee, S.B., Hardcastle, K.C., Wise, D.U., 1994. A method of collecting and analyzing lineaments for regional scale fissured-bedrock aquifer studies. *Ground Water* 32 (4), 884–894.
- Magowe, M., Carr, J.R., 1999. Relationship between lineaments and ground water occurrence in Western Botswana. *Ground Water* 37, 282–286.
- Maréchal, J.C., Dewandel, B., Subrahmanyam, K., 2004. Use of hydraulic test at different scales to characterize fracture network properties in the weathered-fractured layer of hard rock aquifer. *Water Resour. Res.* 40 (W11508), 1–17.
- Mazac, O., Kelly, W.E., Landa, I., 1985. A hydro-geophysical model for relations between electrical and hydraulic properties of aquifer. *J. Hydrol.* 79, 1–19.
- Nahon, D.B., 1991. Introduction to the Petrology of Soils and Chemical Weathering. Ed. Wiley.
- Owen, R., Mikailhov, A., Maziti, A., 2003. Groundwater Occurrence In Crystalline Basement Aquifers A GIS Based Study Of A Borehole Dataset In A Uniform Granitic Terrain In Southern Zimbabwe. published in the volume of WaterNet / Warfsa Symposium, Botswana.
- Pickens, J.F., Grisak, G.E., Avis, J.D., Belanger, D.W., Thury, M., 1987. Analysis and interpretation of borehole hydraulic tests in deep boreholes; principles model development, and applications. *Water Resour. Res.* 23 (7), 1341–1375.
- Sander, P., Minor, T.B., Chesley, M.M., 1997. Groundwater exploration based on lineament analysis and reproducibility tests. *Ground Water* 35 (5), 888–894.
- Sander, P., 2007. Lineament in groundwater exploration: a review of applications and limitations. *Hydrogeol. J.* 15, 71–74.
- Sharma, A., Rajamani, V., 2000. Weathering of gneissic rocks in the upper reaches of Cauvery river, south India: implications to neotectonics of the region. *Chem. Geol.* 166, 203–233.
- Singh, K.P., 2005. Nonlinear estimation of aquifer parameters from surficial resistivity measurements. *Hydrol. Earth Sys. Sci. Discuss.* 2, 917–938.
- Singhal, D.C., Niwas, S., Shakeel, M., Adam, B.M., 1998. Estimation of hydraulic characteristics of alluvial aquifer from electrical resistivity data. *J. Geol. Soc. India* 51, 461–470.
- Niwas, S., de Lima, O.A.L., 2003. Aquifer parameter estimation from surface resistivity data. *Ground Water* 41 (1), 95–99.
- Tardy, Y., 1971. Characterization of the principal weathering types by the geochemistry of waters from some European and African crystalline massifs. *Chem. Geol.* 7, 253–271.
- Taylor, R., Howard, K., 2000. A tectono-geomorphic model of the hydrogeology of deeply weathered crystalline rock: evidence from Uganda. *Hydrogeol. J.* 8 (3), 279–294.
- Wright, E.P., 1992. The hydrogeology of crystalline basement aquifers in Africa. *Geol. Soc. London Spec. Publ.* 66, 1–27.
- Wyns, R., Baltassat, J.M., Lachassagne, P., Legchenko, A., Vairon, J., Mathieu, F., 2004. Application of SNMR soundings for groundwater reservoir mapping in weathered basement rocks (Brittany, France). *Bull. Soc. Geol. Fr.* 175 (1), 21–34.
- Wyns, R., Gourry, J.C., Baltassat, J.M., Lebert, F., 1999. Caractérisation multiparamètres des horizons de subsurface (0–100 m) en contexte de socle altéré. In: BRGM, IRD, UPMC, I. (Ed.), 2ème Colloque GEOFCAN, pp. 105–110. Orléans, France.